

Temperature dependence of the pinning potential in $\text{YBa}_2\text{Cu}_3\text{O}_{7-x}$ superconductors

R. M. Schalk, G. Samadi Hosseinali, and H. W. Weber
Atominstytut der Österreichischen Universitäten, A-1020 Wien, Austria

S. Proyer, P. Schwab, and D. Bäuerle
Institut für Angewandte Physik, Johannes Kepler Universität, A-4040 Linz, Austria

S. Gründorfer
ELIN Energieanwendung, A-1140 Wien, Austria

(Received 7 June 1993; revised manuscript received 30 September 1993)

Voltage-current curves obtained from transport measurements on *c*-axis-oriented thin films of $\text{YBa}_2\text{Cu}_3\text{O}_{7-x}$ allow us to determine the temperature, field, and field-orientation dependence of the pinning potential on the basis of the simple Kim-Anderson model for the thermal activation of flux lines. A strong increase of the pinning potential is found at low temperatures, followed by a field-dependent maximum between 60 and 70 K and a decrease towards the transition temperature T_c . The results are compared to literature data of the pinning potential $U_0(T)$ obtained from relaxation measurements and discussed in terms of thermal activation theory and related models for the current dependence of U_0 . The analysis of the E - J curves, results on the angular dependence of J_c^{ab} , calculations of the pinning potential based on the core contribution, and due consideration of the different nature of the flux lines at low and high temperatures lead to a consistent picture, in which all results are explained in a qualitative way, without the need of invoking recent models on complex pinning interactions and on new phases of the flux-line lattice. It is shown that the pinning potential at low temperatures is of the order of the core contribution of a small number of pancake vortices and therefore intrinsically limited to small values, while at higher temperatures the correlation length along the field direction increases, which naturally leads to higher potentials.

I. INTRODUCTION

In comparison to low- T_c materials, the studies of high-temperature superconductors face a number of additional difficulties. One of the most debated questions is the influence of thermal activation on the flux lines,¹⁻³ which are trapped within a pinning potential. In contrast to conventional superconductors, thermal activation cannot be neglected in any measurement of the irreversible properties of a material. Therefore, it is no longer possible to assess the true critical current density J_c (" J_{c0} "), which is defined as the point, where the pinning potential $U(J)$ disappears.⁴ Hence, in order to determine $J_c(T, B)$ or $U_0(T, B)$ a model for the thermal activation as well as for the nature of the underlying pinning mechanism (i.e., a model for its temperature, field, and current dependence) has to be implemented. An additional problem comes from the pronounced layered structure of most high- T_c materials, which result in a different flux line structure at low and high temperatures.^{5,6} A change of the dimensionality of pinning with temperature becomes possible. Fluctuations of the superconducting order parameter near the phase boundary make it difficult or impossible to assess the reversible material properties (T_c, B_{c2}, κ, H_c), which are needed as input parameters in any pinning model. It was argued, that due to the small size of the coherence length ξ , randomly distributed small defects can only lead to a relevant pinning mechanism, if they act on the flux-line lattice in a collective way.^{7,8}

Therefore, a transition from collective to single vortex pinning has to be considered as well. Even a new phase of the flux-line lattice (vortex glass state⁹) has been suggested to occur at lower temperatures in a weak pinning situation. With regard to thermal activation theory, these uncertainties lead to one major problem, namely, the unknown current dependence of the pinning potential U . In a collective pinning (and also in the vortex glass) model a divergence of $U(J)$ at small currents is predicted, while for single vortex pinning $U(J)$ is determined simply by a superposition of the potential gradient due to the driving force (or the gradient in the flux line density) with the spatial shape of the pinning potential. This situation can be approximated satisfactorily by the linear current dependence of $U(J)$ in the Kim-Anderson model.¹⁻³ Another unknown factor refers to possible spatial distributions of pinning potentials of different depth, i.e., to a certain sample inhomogeneity, which may lead to a varying contribution of different sample domains to the total pinning force, depending on field and temperature.

In summary, the limited number and accuracy of experimental data face a complex theoretical situation. Of course one has to favor the simplest and most comprehensive model for an explanation of the experiment. In this contribution, results from transport measurements on thin films of $\text{YBa}_2\text{Cu}_3\text{O}_{7-x}$ are evaluated in two ways: (1) $J_c^{ab}(\theta, T, B)$ data sets allow us to assess the state of the flux line lattice (two or three dimensional). (2) Fits to the $E(J)$ curves with the Kim-Anderson model

yield $U_0(T, B)$. Both kinds of experimental results can be explained within the framework of single flux-line pinning. A simple phenomenological model based on the layer structure is suggested.

II. MODELS FOR $U(J)$

At first, we wish to briefly describe several models for the current dependence of U , which are used in thermal activation theory. In general, thermal activation leads to a hopping of flux lines (or bundles of flux lines) to a neighboring pinning site. In the presence of a driving force (applied current or flux density gradient) the net velocity of the flux line movement is given by

$$v = x_0 \omega_0 (e^{-U^+/kT} - e^{-U^-/kT}), \quad (1)$$

with the attempt frequency ω_0 (10^5 – 10^{11} s $^{-1}$),¹⁰ and the jump distance x_0 . The resulting electric field $E = B \times v$ can be written as¹¹

$$E(J, T, B) = \rho_c J_{c0} (e^{-U^+/kT} - e^{-U^-/kT}), \quad (2)$$

where $\rho_c(T, B)$ is defined as the resistivity at the critical current density J_{c0} . In the case of a saw-tooth potential shape and for overlapping (dense) pinning centers, Eq. (2) simplifies to

$$E(J, T, B) = 2\rho_c J_{c0} e^{-U_0/kT} \sinh\left[\frac{U_0 J}{kT J_{c0}}\right], \quad (3)$$

because $U^\pm = U_0 \mp \Delta U$, with $\Delta U = U_0 J / J_{c0}$. Note that a nonlinear current dependence of $U^\pm(J)$ can be used only in Eq. (2) and not in Eq. (3). Any smooth periodic potential leads to the following current dependence

$$U^\pm = U_0 \left[1 \mp \frac{J}{J_{c0}} \right]^\mu, \quad (4)$$

with $\mu = 3/2$ for a sinusoidal potential shape.¹² Equations (2) or (3) can be used directly for fitting the E - J data and, hence, for evaluating $U_0(T, B)$ (cf. Chap. 3).

More often, the thermally activated flux-flow (TAFF) approximation¹³ is used. In this case J is small compared to J_{c0} and Eq. (2) is reduced to

$$\rho(T, B) = \frac{2\rho_c U_0}{kT} e^{-U_0/kT}, \quad (5)$$

i.e., linear resistivity. For measurements of the resistive transition in a magnetic field the slope of ρ can be evaluated (in the TAFF regime) as

$$\kappa \frac{\delta \ln \rho}{\delta(1/T)} = -U_{\text{eff}} = -U_0 + T \frac{\delta U_0}{\delta T} + kT - \frac{kT^2}{U_0} \frac{\delta U_0}{\delta T}, \quad (6)$$

where the last two terms can be neglected. In order to obtain U_0 from U_{eff} some general T dependence of U_0 (e.g., $\sim H_c^2 \xi^n$) (Ref. 14) has to be introduced, which usually leads to very high $U_0(T=0)$ values (several eV) (Ref. 15). Such high values are, however, in contradiction to

results from relaxation measurements at low temperatures.

Measurements of the time dependence of the magnetization (and therefore of the induced screening currents) offer another possibility to obtain U_0 . Since there is some confusion about the correct formalism in the literature, the basic equations are given here again (cf. also Hagen and Griessen¹⁶ and Schnack *et al.*¹⁷). Equation (2) can be written for dJ/dt in an equivalent way, with different geometry-dependent prefactors. If backward hopping is neglected ($J \leq J_{c0}$), $J(t)$ is obtained as

$$J(t) = J_{c0} \left[1 - \frac{kT}{U_0} \ln \left[\frac{\tau_i + t}{\tau} \right] \right], \quad (7)$$

with $t \ll \tau'$, $\tau' = \tau/2 \exp(U_0/kT)$ and U_0 independent of J . τ_i is the time elapsed after setting the field, at which the relaxation measurement is started, and τ lies between 10^{-6} and 10^{-12} s. Hence, if $J(t)$ is linear on a logarithmic time scale, the normalized relaxation rate S (not to be confused with $R = d \ln J / d \ln t$) can be calculated from Eq. (7)

$$S = -\frac{1}{J(\tau_i)} \frac{dJ(t)}{d \ln t} = -\frac{1}{J(\tau_i)} \frac{kT J_{c0}}{U_0} \frac{t}{\tau_i + t},$$

or

$$U_0 = \frac{kT}{S} + kT \ln \left[\frac{\tau_i}{\tau} \right] \quad \text{for } t \gg \tau_i. \quad (8)$$

Unfortunately, the exact value of τ is unknown and U_0 can be determined only within the uncertainty of the term $kT \ln(\tau_i/\tau)$. The influence of this term is more pronounced at higher temperatures, but it can be shown from experimental data, that the error bar (determined by the physically meaningful range of τ) is less than $\pm 50\%$ of U_0 .¹⁸ If the experimental procedure is the same for all temperatures (i.e., τ_i unchanged), the shape of $U_0(T)$ can be extracted. A summary of some results derived with this method is shown in Fig. 1 for samples of $\text{YBa}_2\text{Cu}_3\text{O}_{7-x}$ and at fields of 1 T (a) and 4 T (b). Although there is a considerable scatter of data due to several experimental difficulties (e.g., correction for reversible magnetization, field overshoot, and temperature instability), a common feature is clearly emerging, namely, an increase of U_0 with T at low temperatures and a rapid decrease near T_c (if the correction for M_{rev} has been made). The values of U_0 at 4.2 K (1 T) range from 15 to 30 meV, and reach about 150 meV at 77 K, a nearly tenfold increase. In other high- T_c compounds the few available data on $U_0(T)$ also indicate an increase of U_0 with T [e.g., Bi 2:2:1:2, Tl 2:2:1:2, and Tl 1:2:1:2 (Ref. 19), Bi 2:2:2:3 (Ref. 20), Tl 2:2:2:3 (Ref. 21), Tl 1:2:2:3 (Ref. 22)], although the mixture of different phases in the Bi and Tl compounds does not allow a systematic comparison with $\text{YBa}_2\text{Cu}_3\text{O}_{7-x}$ at present. In general, the Tl compounds show a behavior, which is very similar to $\text{YBa}_2\text{Cu}_3\text{O}_{7-x}$, while in the Bi compounds the increase of U_0 seems to be less pronounced.

Several explanations of this significant increase of

$U_0(T)$ can be found in literature. The most tempting one was introduced by Hagen and Griessen,¹⁶ who assumed a distribution of activation energies to exist within the sample. However, a relevant contribution of this effect can be expected only, if large domains ($d \gg \lambda$) with different average pinning potentials are present. In this case the magnetization of different domains can be assumed to relax independently and Eq. (6) yields a separate U_0 for each domain. If $\tau_i > 0$, the domains with small U_0 are more strongly relaxed than domains with larger U_0 already at the beginning of the measurement. With increasing temperature the averaged $\langle U_0 \rangle$, obtained from Eq. (6), is increasingly weighted by the high-energy side of the distribution spectrum and, consequently, $\langle U_0 \rangle$ increases. The distributions needed to explain the behavior displayed in Fig. (1) are quite broad, with a maximum typically around 20–50 meV and a high-energy tail up to several hundred meV. No microscopic evidence for such

a strong inhomogeneity of the samples has been found yet. In addition, as will be discussed below, small sample sizes could limit the possible distribution spectrum in some cases quite severely.

The second argument, stated very often, is related to the current dependence of U . It might be expected that the reduced current density J_c/J_{c0} is smaller at high than at low temperatures during the experimental “time window” of the measurement, and therefore $U_{\text{eff}}(J)$ should be higher. However, it should be pointed out that the current dependence was already included in the derivation of Eq. (6) and the parameter U_0 in this formula depends only on temperature and field. In the case of the much stronger current dependence in the collective creep and in the vortex-glass models, $U(J)$ can be written as^{8,23}

$$U(J) = U_0 [(J_{c0}/J)^\mu - 1]. \quad (9)$$

Therefore, U diverges for $J \rightarrow 0$. For the time dependence of the relaxing current Feigel'man⁸ derived the relation

$$J(t) = J_{c0} \left[1 + \frac{kT}{U_0} \ln \left[\frac{t}{\tau_0} \right] \right]^{-1/\mu}, \quad (10)$$

where again $U_0 = U_0(T, B)$. Fits to relaxation measurements with this equation lead to an increase of U_0 with temperature. Only if $U_{\text{eff}}(J, T, B)$ is introduced into Eq. (10) instead of $U_0(T, B)$ can this dependence be suppressed.²⁴ Again there is no theoretical background for such a step. We also demonstrate in the following that this problem can be solved on the basis of our results on transport measurements on thin films.

III. $U_0(T, B)$ DEPENDENCE IN THIN FILMS

Thin films of $\text{YBa}_2\text{Cu}_3\text{O}_{7-x}$,²⁵ fabricated by pulsed laser deposition on (100) MgO substrates and patterned for transport measurements by standard photolithography and wet chemical etching, were used to obtain the in-plane critical current density $J_c^{ab}(\theta, T, B)$.^{26–28} Unfortunately, thermal problems caused by the very high current densities ($\sim 2 \times 10^{11}$ A/m² at 4.2 K) limit the experimental window, within which the electric field can be monitored, to about one decade ($E_{\text{max}} \sim 20$ $\mu\text{V}/\text{cm}$, $\Delta E_{\text{noise}} \sim 1$ $\mu\text{V}/\text{cm}$). Fits to the data were made at all temperatures and fields on the basis of Eq. (2). The three fit parameters $\rho_c(T, B)$, $U_0(T, B)$, and $J_{c0}(T, B)$ can be reduced to two because the sensitivity of U_0 and J_{c0} in Eq. (2) to the exact value of ρ_c is very weak (at low temperatures a variation of ρ_c by two orders of magnitude changes U_0 only by several percent). As a reasonable approximation for ρ_c , linear extrapolation of the normal-state resistivity is used. The current dependence of $U(J)$ is introduced through Eq. (4) for $\mu=1$ (Kim-Anderson) and $\mu=3/2$ (smooth periodic potential). The values of U_0 and J_{c0} obtained with $\mu=3/2$ were only a few percent larger than the ones obtained with $\mu=1$; the relative field and temperature dependence remains unchanged. Since less calculation time is needed for $\mu=1$, most fits were obtained in this way. The quality of the fits was perfect within the resolution of the measurements. In Fig. 2(a)

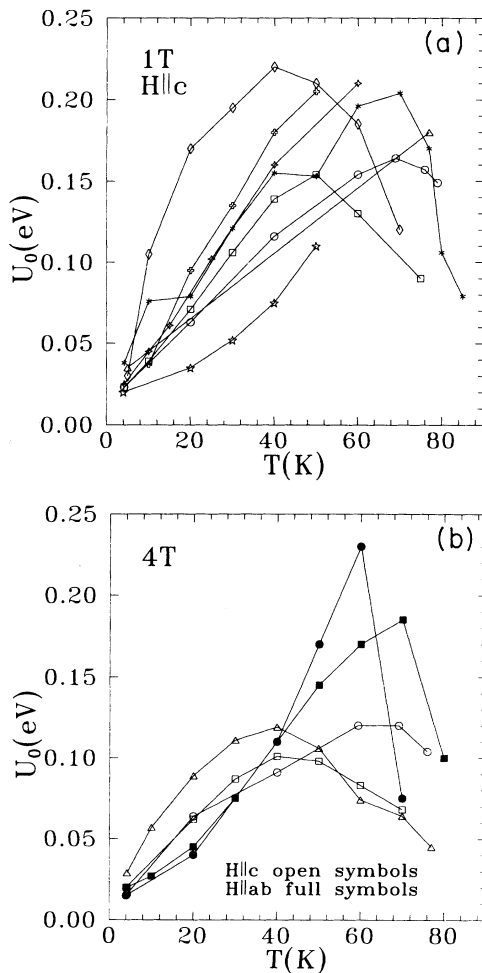


FIG. 1. (a) $U_0(T)$ as determined from magnetization relaxation measurements at an applied field of about 1 T ($\parallel c$). The data were taken from several publications: \diamond ,³⁸ \square ,³⁹ \star ,⁴⁰ \star ,⁴¹ \star ,⁴² \triangle ,⁴³ \star ,⁴⁴ \circ (fit results for film P41831/1). (b) $U_0(T)$ at 4 T. Open symbols are data for $H \parallel c$, full symbols for $H \parallel ab$. References: \bullet ,⁴⁵ \blacksquare and \triangle ,⁴¹ \square ,⁴⁶ and \circ (fit results for film P41831/1).

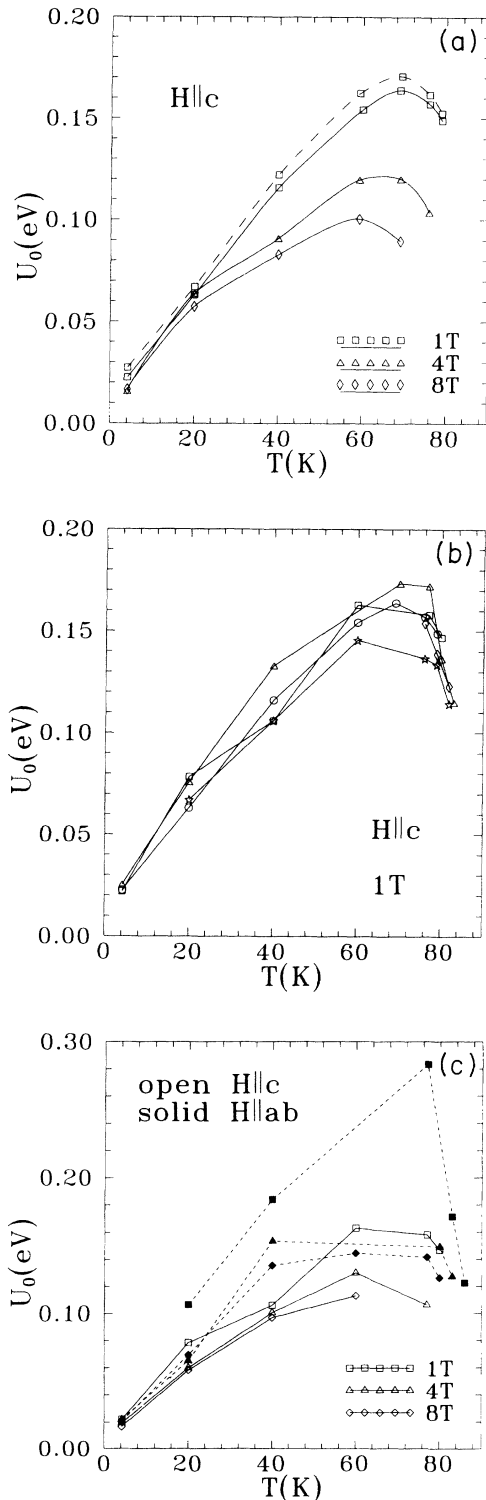


FIG. 2. Temperature dependence of the pinning potential. (a) U_0 for 1, 4, and 8 T ($H||c$) (P41831/1). Note the shift of the maximum to lower temperatures with increasing field. The dashed line (1 T) was obtained using a nonlinear current dependence of U (cf. text). (b) Comparison of $U_0(T)$ for several laser deposited films at 1 T ($H||c$). All films show similar results for U_0 , independently of the magnitude of J_c . (c) $U_0(T)$ for $H||c$ (open symbols) and $H||ab$ (full symbols) (P322/3). At high temperatures the intrinsic pinning mechanism seems to enhance U_0 for $H||ab$.

the resulting temperature dependence of U_0 is summarized for different applied fields. The solid curves represent results for $\mu=1$, the dashed curve shows the result for 1 T and $\mu=3/2$ for comparison. It will be noted, that a strong increase of U_0 with temperature occurs, similar to the results of relaxation measurements in Fig. 1. At an applied field of 1 T the maximum of U_0 , corresponding to an eightfold increase of its value at 4.2 K, occurs at 70 K and shifts to about 60 K at a field of 8 T. In Fig. 2(b), results at 1 T are compared for a number of different films. Although the values of the critical current density in these films varied by a factor of 10, the results for the pinning potential are almost the same. Deviations are mostly due to thermal voltages, which spoil the fits. The increase of U_0 though cannot compensate for the increase of T , i.e., the ratio U_0/kT , which is a measure of the influence of thermal activation, decreases with temperature. As shown in Fig. 3 this ratio becomes smaller at higher temperatures and, hence, thermal activation becomes more severe. Similarly, the ratio of the critical current density J_c , which is defined by a voltage criterion of $10 \mu\text{V}/\text{cm}$, and the fit parameter J_{c0} , which is defined by $U^+(J_{c0})=0$, is also decreasing with increasing temperature (Fig. 4). While the change of J_c/J_{c0} is moderate at intermediate temperatures, it quickly approaches zero near the “irreversibility line,” especially in higher fields.

In order to explain this pronounced increase of $U_0(T)$, we wish to consider a distribution of activation energies at first. This is not an easy task in the case of resistive measurements, since the pattern of current flow in an inhomogeneous material can be very complicated. Griessen²⁹ proposed an approach by assuming that the different domains in the sample can be considered as a network of parallel resistors. According to this model the drop of the electric field across each domain is the same, and domains with higher pinning energies somehow “short circuit” domains with small potential wells, i.e., they carry a higher current density. At higher temperatures, domains with high pinning energies carry

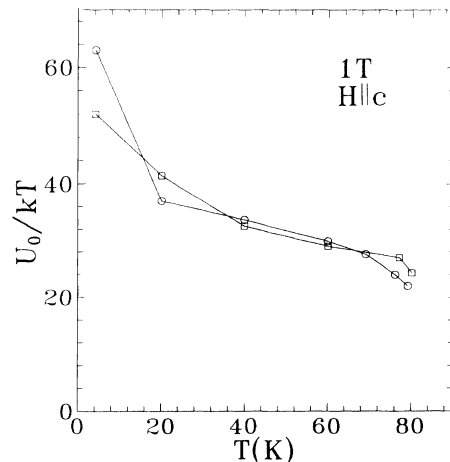


FIG. 3. U_0/kT for two films at 1 T ($H||c$). The influence of thermal activation is enhanced with increasing temperature.

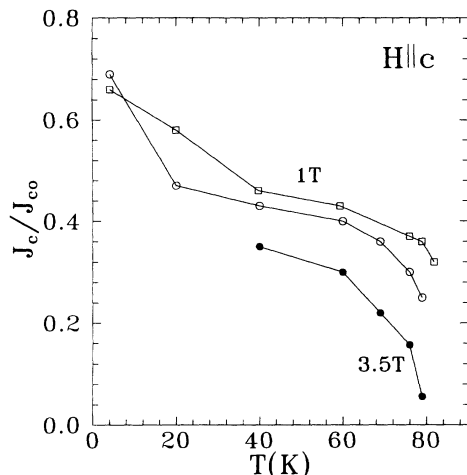


FIG. 4. J_c/J_{c0} at 1 T (two samples) and 3.5 T (one sample) ($H \parallel c$). Note the rapid decrease upon approaching the “irreversibility line” for 3.5 T.

most of the current and the observed averaged potential is increased. Yet it has to be considered that the dimensions of the samples (typically the width of the current bridge for measurements on thin films) limit the extent of the possible distribution spectrum. Griessen assumes that the size of a pinning domain must be at least of the order of ξ . To be physically meaningful, however, we believe that it must be at least of the order of λ , since this is the relevant length, over which the current density can vary considerably. Any inhomogeneous distribution of potential depths within λ is averaged *independently* of temperature. Therefore, a current bridge with a width of typically $10 \mu\text{m}$ could allow for roughly 100 parallel domains ($\lambda \sim 100 \text{ nm}$). Similarly, variations over the length of the bridge ($100\text{--}500 \mu\text{m}$) are again averaged, and the number of effective parallel domains is reduced. In view of this situation it seems doubtful that the observed increase of U_0 by almost one order of magnitude can be attributed to a distribution spectrum of pinning energies. Two further observations are also not in favor of the distribution model. The first is the similarity of the size and shape of $U_0(T)$ for different films. Any large inhomogeneity of pinning energies between different domains should express itself in varying results for U_0 in different parts of the film, especially in view of the small number of possible parallel domains. The second hint against the distribution model is provided by the results on $U_0(T)$, obtained after irradiation of the samples with fast neutrons up to a fluence of $7 \times 10^{21} \text{ m}^{-2}$. Almost no change of J_c and *no* change of U_0 could be found in the irradiated samples. This points to an already optimized defect structure in *all* regions of the sample prior to irradiation. If the low values of activation energies at low temperatures were due to a majority of domains with small potentials, at least some increase of U_0 after the introduction of the several nm-sized neutron defects should occur and the relevant distribution spectrum should be changed. Relaxation measurements after neutron³⁰ and ion³¹ irradiation also show only small changes of the

magnitude of U_0 at low temperatures, even though J_c was increased dramatically. An especially interesting result was obtained recently by Hardy *et al.*³² after irradiation of ceramic $\text{YBa}_2\text{Cu}_3\text{O}_{7-x}$ with 5.3-GeV Pb ions. The introduced defect tracks enhanced J_c at 6 K by a factor of 8 (at 1 T), while U_0 was increased only from 30 to 50 meV. At 77 K, however, U_0 could be increased from 150 to 540 meV. So even after the introduction of a specific strongly pinning defect structure, which is exclusively relevant for pinning, the strange increase of U_0 with T was actually enhanced. Hardy obtained similar results for Tl 2:2:1:2 and Tl 1:2:1:2 single crystals, i.e., a 50% enhancement of U_0 at 6 K and a threefold increase at 25 K in both materials after irradiation with Pb ions.¹⁹ In Bi 2:2:1:2 single crystals he found small activation energies prior to irradiation (10–30 meV) and equal enhancements in the range of 6–25 K (factor of 3–4) after the irradiation. At higher temperatures the radiation-induced decrease of T_c complicates the interpretation of the results. An equivalent picture was found by Neumüller *et al.*,³³ who irradiated polycrystalline melt-textured Bi 2:2:1:2 layers ($d \sim 15 \mu\text{m}$) with 0.5 GeV iodine ions. After the introduction of the ion tracks, U_0 increased only by a factor of 2 at 10 K (from 35 to 70 meV). One has to bear in mind, however, that an estimate of the core pinning potential of the whole columnar defect (diameter 5–10 nm and the length equals the thickness of the sample) results in several eV.

A promising explanation for the strange temperature dependence of the pinning potential in high-temperature superconductors can be based on the layered structure of the superconducting state, and the corresponding flux line structures, which are different from conventional superconductors.^{5,6} Keeping this in mind we first wish to calculate numerically the core contribution for single flux-line pinning and different defect sizes, as core pinning is dominant in high- κ materials. The layer structure is taken into account in the following way: (1) The field is applied parallel to the c axis and the flux line splits up into a stack of pancake vortices. (2) The relevant area for core pinning perpendicular to the field is given by a disk of radius ξ_{ab} (i.e., the cross section of a pancake vortex) within the superconducting layer, which is assumed to be of thickness $s=0.4 \text{ nm}$. (3) The interlayer distance d (which is 0.8 nm) is reduced by the size of ξ_c ($d'=d-\xi_c$). Hence, for $\xi_c=d$ the layer structure is suppressed and a regular three-dimensional (3D) flux line is formed. If we now consider the maximum core volume of one pancake vortex, it will grow in three dimensions with increasing temperature because ξ_{ab} as well as ξ_c increase with T . The shaded areas in Fig. 5 illustrate the core volume of a stack of several pancakes at two different temperatures. We now assume, that a cylindrical defect is placed onto the center of a superconducting layer in such a way that the cylinder axis is parallel to the c direction. The diameter of the defect is assumed to be always larger than $2\xi_{ab}$ and its height to be equal to a certain length in c direction, which corresponds to multiples of the superconducting layer thickness s and represents a “correlation” length L_c in the field direction.

This special defect geometry is chosen because the intersection of the defect with the layered pancake structure can be calculated most easily in this geometry. Similar results would be obtained for other defect geometries. To calculate the core pinning energy numerically, we take $\mu_0 H_c(0) = 1$ T, $\xi_{ab}(0) = 1.5$ nm, $\xi_c(0) = 0.3$ nm, $H_c(T) = H_c(0)(1 - t^2)$, and $\xi(T) = \xi(0)/\sqrt{1 - t}$, with $t = T/T_c$. The temperature dependence of U_{core} is plotted for different defect sizes (diameter of the defect $> 2\xi_{ab}$; height: 1.2, 5, 10, 15, or 20 nm) in Fig. 6. The solid lines, therefore, indicate situations, where one (thick solid line) or more pancake vortex cores are found within one defect. In the case of one pancake vortex, a slight increase of U_0 at low temperatures and a peak at 40 K are obtained because the increase of the core volume in three dimensions exceeds the decrease of H_c at low temperatures. This effect is by far not large enough to account for the experimentally observed increase of U_0 , which has been included for one typical case (at 1 T) as the dashed line in Fig. 6. A comparison of the experimental $U_0(T)$

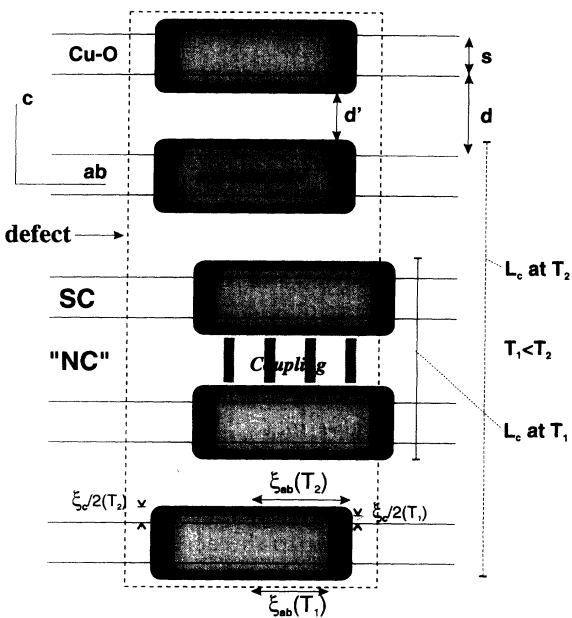


FIG. 5. Schematic diagram of a layered superconductor (parameters for $\text{YBa}_2\text{Cu}_3\text{O}_{7-x}$). s denotes the thickness of the superconducting Cu-O layers and d the interlayer distance. d' is the effective interlayer distance, i.e., $d - \xi_c$. The field is applied parallel to the c axis, and the flux line splits up into pancake vortices (shaded areas). The pancake cores are assumed to be cylindrical in shape. The coherence lengths and the corresponding maximum core volumes, which have to be added up to obtain the pinning potential, are shown for two temperatures (light and dark shading). d' , and, therefore, the effective spacing of the pancake vortices in different layers, is reduced with increasing temperature. At higher temperatures the coupling between pancake vortices and, hence, the correlation length L_c of pinning, is increased. In the presence of a defect a certain number of pancakes, given by the correlation length, are displaced simultaneously. The observed pinning potential is made up by the sum of core volumes of these pancake vortices.

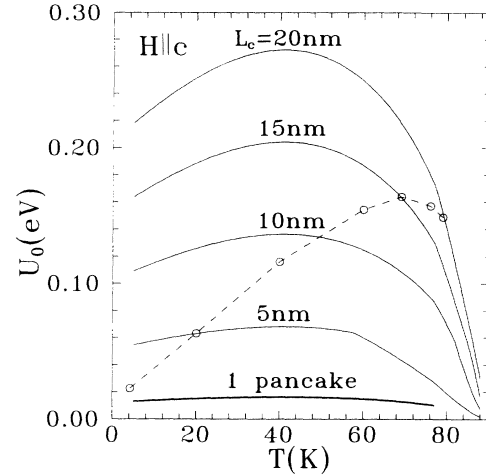


FIG. 6. Numerical calculation of the core pinning potential for different correlation lengths L_c (and consequently for different numbers of pancake vortices being displaced together) along the field direction (solid lines). The thick solid line shows the contribution of the core volume of one pancake vortex. For comparison the experimental data on P41831/1 at 1 T are shown as well (dashed line).

with the various calculated curves implies that the observed pinning potential is close to the contribution of a single pancake vortex at low temperatures, whereas at higher temperatures a considerably larger pinning volume (or correlation length L_c in the field direction) is necessary to account for the large pinning potentials (e.g., $L_c = 15$ –20 nm at 77 K, which corresponds to about 12–17 pancake vortices). Hence, at low temperatures individual pancake vortices are displaced almost independently in the presence of a defect, while with increasing temperature the number of pancake vortices, which are displaced together is increasing. We therefore propose that the large change of the correlation (or displacement) length with temperature must be a direct consequence of a transition in the flux-line structure from a stack of pancake vortices at low temperatures to a regular flux line at high temperatures.

Support for this assumption is provided by theory, although most of these considerations are not directly applicable to $\text{YBa}_2\text{Cu}_3\text{O}_{7-x}$. It is known that in layered and anisotropic systems the tilt modulus c_{44} is considerably reduced. According to the Lawrence-Doniach (LD) model (ignoring Josephson coupling and considering independent vortices) $c_{44}^{\text{layer}} = (d/\lambda_{ab})^2 c_{44}^{\text{iso}}$.³⁴ Therefore, c_{44} is smaller in most high-temperature superconductors than in an isotropic superconductor by factors of the order of 10^4 – 10^6 . Recent calculations on the line tension and the line energy of a flux line in the case of strong pinning by columnar defects parallel to the c direction showed that the depinning length was inversely proportional to the anisotropy factor Γ .³⁵ Therefore, the displacement length in highly anisotropic materials (especially Bi 2:2:1:2, Bi 2:2:2:3, and Tl 2:2:2:3) may become smaller than the layer spacing d and the displacement of individual pancake vortices may be possible. Measurements of the angular dependence of J_c (Ref. 36) in these

materials and the stronger influence of thermal activation at high temperatures point in this direction. Consequently small pinning potentials will result, even at high temperatures and for large defect volumes, because the pinning potential for thermal activation is still determined only by the contribution of one pancake vortex. Unfortunately, no theory is available, which provides a link between the LD theory and the regular 3D anisotropic Ginzburg-Landau theory. Therefore, no detailed predictions about the behavior of a transition from pancake vortices in weakly coupled superconducting layers with $\xi_c < d$ to a 3D vortex lattice with $\xi_c \geq d$ can be made. Such a transition regime is expected for $\text{YBa}_2\text{Cu}_3\text{O}_{7-x}$, i.e., a crossover from quasi-2D to 3D flux line behavior. Detailed calculations of the temperature dependence of the displacement length are still missing. In general, however, enhanced coupling between pancake vortices at higher temperatures must lead to an increase of the depinning length.

Evidence for a pancake structure in $\text{YBa}_2\text{Cu}_3\text{O}_{7-x}$ has been derived from measurements of the angular dependence of J_c^{ab} in our films.^{27,28} It was shown, that $J_c^{ab}(\theta)$ at 4.2 K depended only on the field component in the c direction for fields not too close to the ab plane, i.e., only vortex movements within the ab plane were possible (2D scaling of J_c). With increasing temperature the coupling between adjacent pancake vortices becomes stronger and the correlation length along the c axis, and therefore U_0 , has to increase. The question of why changes of U_0 occur at temperatures between 4.2 and 40 K, where the coherence length ξ_0 changes only very little, is still not quite answered. However, there is evidence from the angular dependence of J_c that significant changes in the coupling between the pancake vortices occur. It was noted^{27,28} that small systematic deviations from 2D scaling already occur at 20 K and that these deviations are so large at 40 K, that the 2D model fails completely. Hence, even with the lack of a theoretical basis, there is strong phenomenological evidence for a considerable change in the coupling between pancake vortices at low temperatures (4.2–40 K). On the high temperature side a maximum of U_0 must occur because the strong decrease of H_c near T_c starts to dominate and U_0 decreases. For temperatures above 60 K and for fields close to the ab plane, pronounced intrinsic pinning phenomena can be observed (e.g., a lockin of the flux line into the ab plane) and the flux-line structure can be assumed to be almost 3D in nature.

If the above model is correct, the small pinning potential at low temperatures is an intrinsic property of high-temperature superconductors and cannot be strongly improved by introducing additional large defects. This is confirmed by various irradiation experiments, especially with high-energy ions. The introduction of large defects should have its strongest effect at high temperatures, where the correlation of the pinned flux line over the whole defect becomes possible, i.e., an even stronger increase of U_0 is expected and also observed.³² A similar effect is expected with respect to the intrinsic pinning mechanism, defined as the pinning of the 3D flux line by the interlayer plane. If intrinsic pinning occurs, the large

correlation length along the flux line should result in higher pinning potentials, especially in the case, where a complete lockin of the flux lines into the ab plane occurs. In order to investigate this influence, fits were made to the E - J curves for $H||ab$ and the values of $U_0(T)$ compared to the results for $H||c$ [Fig. 2(c)]. It will be noted that the pinning potentials at 4.2 K are almost the same for both orientations, while with increasing temperature the U_0 values for $H||ab$ become increasingly larger than those for $H||c$ [see also Fig. 1(b)]. This is again in agreement with the above model, because in the 2D regime of weakly coupled pancakes the pinning potential is always governed by pancake displacement within the ab plane (due to crystal imperfections there is always a small internal c component of the applied field). Thin films with a more pronounced lockin behavior than observed in the present samples should show an even stronger enhancement of U_0 ($H||ab$).

In principle, changes in the transverse correlation length R_c (perpendicular to the field) also have to be considered, especially in collective pinning models. It seems reasonable, however, that collective pinning does not occur in $\text{YBa}_2\text{Cu}_3\text{O}_{7-x}$ even at 4.2 K, since the observed current densities (up to 5×10^{11} A/m²) are not far from the pair breaking limit, which can be calculated from experimental H_{c1} data. With $H_{c1}(0)$ in the range from 30 to 300 mT we obtain an upper limit for J_c of 2×10^{11} to 5×10^{12} A/m². In a collective model, however, the short-range order of the flux line lattice limits the possible vortex displacements (and therefore the microscopic pinning forces) and J_c is always far from its maximum value. On the contrary, in very clean (defect free) single crystals, which have become available only very recently,³⁷ collective pinning effects may have to be considered.

Finally we wish to discuss the field dependence of U_0 (Fig. 7), which was evaluated for some films at higher temperatures, where the experimental errors due to thermal voltages are small. A strong decrease of U_0 at low fields (< 1 T) and an almost linear decrease at higher fields was found at temperatures between 60 and 90 K. A

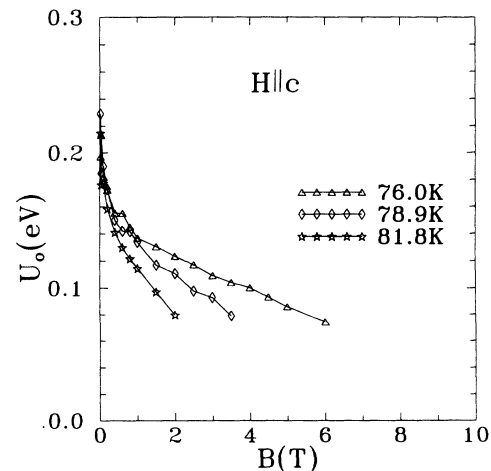


FIG. 7. Field dependence of U_0 at high temperatures. A linear extrapolation to zero leads to an estimate of B_{c2} .

linear extrapolation of U_0 to zero may allow one to determine B_{c2} . In the high-field regime near B_{c2} , the elementary pinning force and the pinning potential for strong pinning of individual vortices are proportional to the magnitude of the order parameter, which in turn varies as $(1-B/B_{c2})$. Therefore, according to this Ginzburg-Landau argument a linear decrease of U_0 near B_{c2} is expected. Linear extrapolation of our data (Fig. 7) leads to a slope of -1 T/K ($H_{c2}||c$), which is clearly smaller than the result deduced from magnetization measurements on single crystals (~ -2 T/K). Higher disorder and lower T_c values in the thin films may explain this difference. However, the currently available data are not sufficiently accurate for a more detailed analysis of this aspect (too noisy at these high fields and temperatures). Further experimental work with improved voltage resolution will be needed to assess the field dependence of U_0 at high magnetic fields and to check for the viability of the proposed method to determine B_{c2} .

IV. SUMMARY

It has been shown in the present contribution that the strange behavior of $U_0(T)$, i.e., its strong increase with temperature, in $\text{YBa}_2\text{Cu}_3\text{O}_{7-x}$ and in other high-temperature superconductors can be considered as an intrinsic property of the flux-line lattice, which is caused by the influence of the layer structure on the superconducting state. If one considers a flux line as consisting of a stack of weakly coupled pancake vortices at low temperatures, the correlation volume for pinning can be assumed to be of the order of one pancake vortex (or a small number of pancake vortices.) This is supported by the small magnitude of the observed pinning potential, as deter-

mined from relaxation measurements and also from fits to the E - J curves of transport measurements on thin films. Calculations of the core-pinning potential lead to a similar value, when the contributions of one or two pancake vortices are taken at 4.2 K. This picture is also in agreement with results on the angular dependence of J_c^{ab} , which shows 2D scaling at this temperature. At higher temperatures the coupling between pancake vortices seems to be steadily enhanced, even in the range from 4.2 to 40 K, where the coherence length changes only very little. The strong increase of the pinning potential by almost one order of magnitude is attributed to a strong enlargement of the correlation length for pinning along the field (c) direction. This assumption is again in agreement with the $J_c(\theta)$ data, which show quickly increasing deviations from 2D scaling with increasing temperature. In the temperature range from 60 K to T_c , a 3D picture of the flux line structure is more appropriate to explain the intrinsic pinning phenomena near $H||ab$ and the higher values of the pinning potential. Other models for the description of this special behavior, like the assumption of a distribution of activation energies in an inhomogeneous material or a collective pinning picture, are not able to account for all of the observed features in a comprehensive way.

ACKNOWLEDGMENTS

This work has been supported in part by the EC SCIENCE program under Contract No. SC1-0389. Technical support by H. Niedermaier is gratefully acknowledged. Three of us (S.P., P.S., and D.B.) wish to thank the "Forschungsfonds für die Gewerbliche Wirtschaft in Österreich" for financial support.

-
- ¹P. W. Anderson, *Phys. Rev. Lett.* **9**, 309 (1962).
²P. W. Anderson and Y. B. Kim, *Rev. Mod. Phys.* **36**, 39 (1964).
³Y. B. Kim, C. F. Hempstead, and A. R. Strnad, *Phys. Rev.* **131**, 2486 (1963).
⁴A. P. Malozemoff, T. K. Worthington, Y. Yeshurun, and F. Holtzberg, *Phys. Rev. B* **38**, 7203 (1988).
⁵J. R. Clem, *Phys. Rev. B* **43**, 7837 (1991).
⁶L. N. Bulaevskii, M. Ledvij, and V. G. Kogan, *Phys. Rev. B* **46**, 366 (1992).
⁷M. V. Feigel'man, V. B. Geshkenbein, A. I. Larkin, and V. M. Vinokur, *Phys. Rev. Lett.* **63**, 2303 (1989).
⁸M. V. Feigel'man, V. B. Geshkenbein, and V. M. Vinokur, *Phys. Rev. B* **43**, 6263 (1991).
⁹M. P. A. Fisher, *Phys. Rev. B* **62**, 1415 (1989).
¹⁰M. Tinkham, *Introduction to Superconductivity* (McGraw-Hill, New York, 1975), p. 175.
¹¹E. H. Brandt, *Supercond. Sci. Technol.* **5**, S25 (1992).
¹²R. Griessen, *Physica C* **172**, 441 (1991).
¹³P. H. Kes and J. van den Berg, in *Studies of High Temperature Superconductors*, edited by A. V. Narlikar (Nova Science, New York, 1990), Vol. 5, p. 83.
¹⁴M. Tinkham, *Introduction to Superconductivity* (McGraw-Hill, New York, 1975).
¹⁵T. T. M. Palstra, B. Batlogg, R. B. van Dover, L. F. Schneemayer, and J. V. Waszczak, *Phys. Rev. B* **41**, 6621 (1990).
¹⁶C. W. Hagen and R. Griessen, in *Studies of High Temperature Superconductors*, edited by A. V. Narlikar (Nova Science, New York, 1989), Vol. 3, p. 159.
¹⁷H. G. Schnack, R. Griessen, J. G. Lensink, C. J. van der Beek, and P. H. Kes, *Physica C* **197**, 337 (1992).
¹⁸P. Fischer, H.-W. Neumüller, B. Roas, H. F. Braun, and G. Saemann-Ischenko, *Solid State Commun.* **72**, 871 (1989).
¹⁹V. Hardy, thesis, Universite de Caen, 1992.
²⁰M. Mittag, R. Job, and M. Rosenberg, *Physica C* **174**, 101 (1991).
²¹V. K. Chan and S. H. Lion, *Phys. Rev. B* **45**, 5547 (1992).
²²M. Mittag, M. Rosenberg, B. Himmerich, and H. Sabrowsky, *Supercond. Sci. Technol.* **4**, 244 (1991).
²³D. S. Fisher, M. P. A. Fisher, and D. A. Huse, *Phys. Rev. B* **43**, 130 (1991).
²⁴W. Schindler, thesis, Friedrich-Alexander-Universität Erlangen-Nürnberg, 1992.
²⁵D. Bäuerle, *Appl. Phys. A* **48**, 527 (1989).
²⁶R. M. Schalk, H. W. Weber, Z. H. Barber, C. E. Davies, J. E. Evetts, R. E. Somekh, and D. H. Kim, *Supercond. Sci. Technol.* **5**, S224 (1992).
²⁷R. M. Schalk, H. W. Weber, Z. H. Barber, P. Przyslupski, and J. E. Evetts, *Physica C* **199**, 311 (1992).
²⁸R. M. Schalk, G. Samadi Hosseinali, H. W. Weber, Z. H.

- Barber, P. Przyslupski, J. E. Evetts, A. Pönninger, P. Schwab, S. Proyer, A. Kochemasov, and D. Bäuerle, *Cryogenics* **33**, 369 (1993).
- ²⁹R. Griessen, *Physica C* **175**, 315 (1991).
- ³⁰W. Schindler, *J. Appl. Phys.* **70**, 1877 (1991).
- ³¹H. W. Neumüller, G. Ries, W. Schmidt, W. Gerhäuser, and S. Klaumünzer, *Supercond. Sci. Technol.* **4**, S370 (1991).
- ³²V. Hardy, D. Groult, J. Provost, and B. Raveau, *Physica C* **190**, 289 (1992).
- ³³H. W. Neumüller, W. Gerhäuser, G. Ries, P. Kummeth, W. Schmidt, S. Kalumünzer, and G. Saemann-Ischenko, *Cryogenics* **33**, 14 (1993).
- ³⁴K. H. Fischer, *Physica C* **178**, 161 (1991).
- ³⁵E. H. Brandt, *Europhys. Lett.* **18**, 635 (1992).
- ³⁶P. Schmitt, P. Kummeth, L. Schultz, B. Roas, and G. Saemann-Ischenko, *Supercond. Sci. Technol.* **5**, S101 (1992).
- ³⁷H. Safar, P. L. Gammel, D. A. Huse, and D. J. Bishop, *Phys. Rev. Lett.* **69**, 824 (1992).
- ³⁸L. W. Song, M. Yang, E. Chen, and Y. H. Kao, *Phys. Rev. B* **45**, 3083 (1992).
- ³⁹J. G. Lensink, thesis, Vrije Universiteit te Amsterdam, 1993.
- ⁴⁰W. Schindler, *J. Appl. Phys.* **70**, 1877 (1991).
- ⁴¹H. Küpfer, C. Keller, R. Meier-Hirmer, K. Salama, V. Selvamanickam, and G. Tartaglia, *IEEE Trans. Magn. MAG-27*, 1369 (1992).
- ⁴²J. G. Lensink, R. Griessen, H. P. Wiesinger, F. M. Sauerzopf, H. W. Weber, and G. W. Crabtree, *Physica C* **185-189**, 2287 (1991).
- ⁴³P. Fischer, H. W. Neumüller, B. Roas, H. F. Braun, and G. Saemann-Ischenko, *Solid State Commun.* **72**, 871 (1989).
- ⁴⁴D. Shi and S. Salem-Sugui, Jr., *Phys. Rev. B* **44**, 7647 (1991).
- ⁴⁵C. Keller, H. Küpfer, A. Gurevich, R. Meier-Hirmer, T. Wolf, and R. Flükiger, *J. Appl. Phys.* **68**, 3498 (1990).
- ⁴⁶M. Wacencosky, thesis, Technische Universität Wien, 1993.

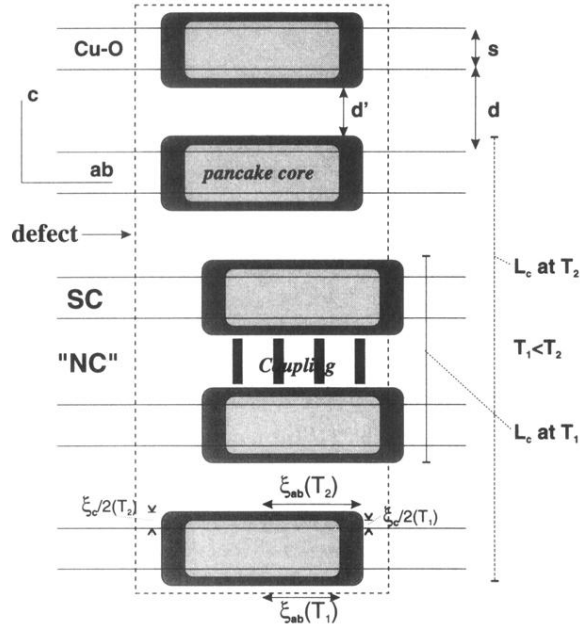


FIG. 5. Schematic diagram of a layered superconductor (parameters for $\text{YBa}_2\text{Cu}_3\text{O}_{7-x}$). s denotes the thickness of the superconducting Cu-O layers and d the interlayer distance. d' is the effective interlayer distance, i.e., $d - \xi_c$. The field is applied parallel to the c axis, and the flux line splits up into pancake vortices (shaded areas). The pancake cores are assumed to be cylindrical in shape. The coherence lengths and the corresponding maximum core volumes, which have to be added up to obtain the pinning potential, are shown for two temperatures (light and dark shading). d' , and, therefore, the effective spacing of the pancake vortices in different layers, is reduced with increasing temperature. At higher temperatures the coupling between pancake vortices and, hence, the correlation length L_c of pinning, is increased. In the presence of a defect a certain number of pancakes, given by the correlation length, are displaced simultaneously. The observed pinning potential is made up by the sum of core volumes of these pancake vortices.